Multi-specific DARPin® therapeutics demonstrate very high potency against mutated SARS-CoV-2 variants *in vitro*

Sylvia Rothenberger[1,2,*], Marcel Walser[3,*], Francesca Malvezzi[3], Jennifer Mayor[1,2], Sarah Ryter[1], Hector Moreno[2], Nicole Liechti[1], Silvan Hälg[4], Andreas Bosshart[3], Chloe Iss[3], Valérie Calabro[3], Andreas Cornelius[3], Tanja Hospodarsch[3], Alexandra Neculcea[3], Thamar Looser[3], Susanne Mangold[3], Christian Reichen[3], Filip Radom[3], Keith M. Dawson[3], Seth Lewis[3], Daniel Steiner[3], Patrick Amstutz[3], Olivier Engler[1,**], Michael T. Stumpp[3,5,**]

* These first authors contributed equally to this work

** These senior authors contributed equally to this work

[1]Spiez Laboratory, Austrasse, 3700 Spiez, Switzerland

[2]Institute of Microbiology, University Hospital Center and University of Lausanne, Rue du Bugnon 48, 1011 Lausanne, Switzerland

[3]Molecular Partners AG, Wagistrasse 14, 8952 Zurich-Schlieren, Switzerland

[4]Swiss Tropical and Public Health Institute, Department Epidemiology and Public Health, Basel, Switzerland. University of Basel, Basel, Switzerland.

[5]To whom correspondence should be addressed:

Michael T. Stumpp

+41 44 755 77 00

info@molecularpartners.com

Keywords: SARS-CoV-2, COVID-19, corona virus, mutations, ensovibep, emerging variants, antiviral therapy, viral passaging, DARPin® drug, ankyrin repeat protein, multi-specific, E484K, N501Y, B.1.1.7, B.1.351, MP0420, MP0423

DARPin® is a registered trademark owned by Molecular Partners AG

Abstract

The SARS-CoV-2 virus responsible for the COVID-19 pandemic has so far infected more than 100 million people globally, and continues to undergo genomic evolution. Emerging SARS-CoV-2 variants show increased infectivity and may lead to resistance against immune responses of previously immunized individuals or existing therapeutics, especially antibody-based therapies.

Several monoclonal antibody therapeutics authorized for emergency use or in development start to lose potency against various SARS-CoV-2 variants. Cocktails of two different monoclonal antibodies constitute a promising approach to protect against such variants as long as both antibodies are potent, but come with increased development complexity and therefore cost. As an alternative, we developed two multi-specific DARPin® therapeutics, each combining three independent DARPin® domains binding the SARS-CoV-2 spike protein in one molecule, to potently neutralize the virus and overcome virus escape.

Here, we show in a panel of *in vitro* studies that both multi-specific DARPin® therapeutics, ensovibep (MP0420) and MP0423, are highly potent against the new circulating SARS-CoV-2 variants B.1.1.7 (UK variant) and B.1.351 (South African variant) and the most frequent emerging mutations in the spike protein. Additionally, viral passaging experiments show potent protection by ensovibep and MP0423 against development of escape mutations. Furthermore, we demonstrate that the cooperative binding of the individual modules in a multi-specific DARPin® antiviral is key for potent virus inhibition and protection from escape variants. These results, combined with the relatively small size and high production yields of DARPin® molecules, suggests ensovibep and MP0423 as superior alternatives to monoclonal antibody cocktails for global supply and demonstrate the strength of the DARPin® platform for achieving potent and lasting virus inhibition for SARS-CoV-2 and possibly other viruses.

Introduction

After more than a year of the COVID-19 pandemic, new circulating variants of SARS-CoV-2 have been described that show resistance against the immune response of previously immunized individuals[1,2] or available therapeutics[3,4]. In many regions around the globe, governments are implementing lock-down measures to contain rapidly spreading SARS-CoV-2 spike variants associated with increased transmissibility[5]. Recently identified variants in the UK (B.1.1.7 lineage), South Africa (B.1.351 lineage)[6] and Brazil (P.1. lineage)[2] share mutations on the spike protein, which have evolved independently. Amongst those, mutations K417E/N/T, E484K and N501Y are of major concern, as these residues are associated with a change in receptor binding, and thus increased transmissibility and/or immune escape of the virus[3,7,8].

Other mutations confer resistance against monoclonal antibody therapeutics, including N439K, where independent lineages were originally detected in Scotland, subsequently in Romania and then spread in many countries such as the USA[3]. Further amino acid changes, which may reduce therapeutic options are Y453F, which evolved in Danish mink farms[9], and less common mutations, such as G446V, G476S, T478I, P479S, V483A, F486V, F490S and Q493K, originally described by Baum et al.[10]. Additional mutations which occur globally at high frequencies such as A222V, S477N, D614G and Q675H[11,12] are considered less of a concern to date.

To circumvent the loss of potency of single monoclonal neutralizing antibodies, antibody cocktails were generated, providing a higher resistance against escape mutations[10,13]. However, this strategy is associated with increased manufacturing costs and limited global supply capacities[14].

We have applied our DARPin® platform that allows fast generation and cost-effective production of multi-specific therapeutics to generate anti-SARS-CoV-2 multi-specific DARPin® antivirals, with very high neutralizing potencies, which were described previously[15]. In brief, DARPin® molecules are structurally completely different from antibodies and consist of a single chain of linked DARPin® domains; in this case the molecules have two N-terminal human serum albumin (HSA) binding domains for systemic half-life extension and three spike protein binding domains at the C-terminus. The relatively small size of these multi-specific DARPin® antivirals, in the range of 75-85 kDa, in conjunction with the high thermal stability, solubility and very high production yields make these molecules an attractive therapeutic alternative to antibody cocktails.

Two of these DARPin® antivirals, ensovibep and MP0423, are currently in clinical and pre-clinical development. The viral inhibition mode of ensovibep is based on three distinct DARPin® domains targeting the Receptor Binding Domain (RBD) while MP0423 has three DARPin® domains directed to three different domains of the spike protein: the RBD, the N Terminal Domain (NTD) and the S2 domain.

The tripartite binding and RBD-independent neutralization mechanism allow the MP0423 molecule to lose binding to any of its domains while maintaining a high neutralizing potency.

Here, we demonstrate that the two multi-specific DARPin® designs confer protection against a panel of relevant spike mutations as well as two SARS-CoV-2 variants recently identified in the UK (lineage B.1.1.7, del69-70, del145, N501Y, A570D, D614G, P681H, T716I, S982A, D1118H) and South Africa (early evolved variant of lineage B.1.351; D80A, D215G, E484K, N501Y, A701V). In addition, we show in a viral passaging experiment that the multi-specific DARPin® antivirals' protection against development of viral escape mutants is comparable to that of the best characterized and efficacious monoclonal antibody cocktails to date[10]. These data confirm the tripartite design as critical against emerging mutations and strongly validate the further development of ensovibep and MP0423.

Results

Ensovibep and MP0423 are highly potent against the recently identified SARS-CoV-2 UK variant B.1.1.7 and South African variant B.1.351 as well as almost all tested spike protein point mutations

The spike protein of SARS-CoV-2 mediates cell entry through binding to the human ACE2 receptor. SARS-CoV-2 is also capable of infecting non-primate hosts, such as felines and minks[16]. The promiscuity of a multi-host life style is often an indicator of early, still sub-optimal adaptation of the virus to its new host. This suggests inherent dynamic plasticity and potential for further human adaptation. The receptor-binding domain (RBD) in the spike protein forms the interface with ACE2. Site mutagenesis scanning and structure analysis revealed critical residues for this interaction, i.e. L455, F456, A475, F486, F490 and Q493[7,17]. Notably, single amino acid substitutions N439R, L452K, NT470, E484P, Q498Y and N501T have been shown to increase the affinity for human ACE2[7]. Consistent with these experimental findings, mutations N439K and N501Y appeared in rapidly spreading SARS-CoV-2 spike variants in association with facilitated receptor binding and increased transmissibility[3,8,18]. The RBD domain is also immunogenic, and among others residues, K444, E484, and F486 have been shown to be critical for the binding of neutralizing antibodies[13].

In the present study we analyzed the impact of selected critical residues on the neutralization capacity of ensovibep and MP0423 (Figure 1). To assess the potency of the mono-specific and multi-specific DARPin® molecules, we used VSV-based pseudoviruses carrying the SARS-CoV-2 wild-type or mutant spike protein at their surface. These pseudoviruses were used in neutralization tests with multi-specific DARPin® molecules ensovibep and MP0423 or control neutralizing antibodies REGN10933 and REGN10987. A summary of the calculated IC_{50} values are reported in Table 1a and Table 1b.

The results show that ensovibep can neutralize variants of the UK originated lineage B.1.1.7 (del69-70, del145, N501Y, A570D, D614G, P681H, T716I, S982A, D1118H) and the South African originated lineage B.1.351 (D80A, D215G, E484K, N501Y, A701V) as efficiently as the wild-type virus with IC_{50} values in the low single-digit ng/mL range. While MP0423 remained highly potent against the B.1.351 variant, a slight potency loss to 70 ng/mL (i.e. ~20-fold lower than wild-type) was observed against the UK variant B.1.1.7. It is interesting to note that the RBD binder of MP0423 (i.e. RBD-2) retained the same neutralization ability for B.1.1.7 compared to the wild type. Since the inactivation of the NTD binder of MP0423 does not affect the potency of the molecule (Suppl. Figure 2), the observed potency drop is thought to be caused by the exposed mutations in the S2 domain (potentially P681H and T716I) alone or in combination with the NTD mutations. The structural determinants responsible for this potency drop are currently under investigation to confirm this hypothesis.

Both multi-specific DARPin® antivirals, ensovibep and MP0423, protected well against all individual mutations tested, with the notable exception of F486V for ensovibep and all three mono-valent DARPin® RBD binders.

As F486 is a critical residue for ACE2 binding, selective pressure on the virus favors its conservation, thus maintaining an important anchoring element for the binding of ensovibep. The major impact of this mutation on ensovibep is not surprising, as previous structural analysis identified F486 as a core interacting residue for the three related but different RBD binders[15]. Consequently, the mutation F486V destabilizes the binding of the entire tri-specific ensovibep molecule to the spike protein.

Taken together, our analysis confirms that the multi-specific DARPin® molecules are highly potent against spike proteins carrying the most frequently observed mutations as well as mutations known to impact the binding of neutralizing antibodies, as expected from the multi-specific design.

Passaging of SARS-CoV-2 under therapeutic pressure from DARPin® antivirals and monoclonal antibodies

Previous studies have shown that viral escape mutants may rapidly appear under selective pressure of a therapy[1,13]. We used a viral passaging model adapted from Baum et al.[10], to estimate the risk of viral escape from therapeutic pressure of ensovibep and MP0423 and of a cocktail of the two Regeneron monoclonal antibodies REGN10933 & REGN10987, in comparison to the mono-valent DARPin® binder RBD-2 and to the monoclonal antibodies S309, REGN10933 and REGN10987 applied as single molecules.

1.5×10^6 pfu of a French SARS-CoV-2 isolate (with the following differences to the Wuhan wild-type: V367F; E990A) were serially passaged in the presence of increasing concentrations of DARPin® and antibodies (Figure 2A, Figure 2B). Resistant escape variants were further selected by passaging the supernatant of cultures showing significant virus-induced cytopathic effect (CPE) under the selection pressure of the highest therapeutic concentration onto fresh cells while maintaining the selective pressure of increasing concentrations of therapeutic antivirals. After the first incubation cycle of four days (passage 1) the mono-valent DARPin® binder RBD-2 and the multi-specific DARPin® antivirals, as well as the antibody antivirals REGN10933 and the antibody cocktail (REGN10933 & REGN10987) conferred protection at the same concentration of 0.4 µg/mL. The monoclonal antibody S309 was less efficient, requiring a higher concentration (10 µg/mL) for protection and the monoclonal antibody REGN10987 was not protective up to the highest concentration tested of 50 µg/mL. Under continuous selective pressure through passage 2 to 4, the monovalent DARPin® binder RBD-2, and the individual monoclonal antibodies REGN10987 and REGN10933 lost the capacity to protect cells, which manifested in complete CPE up to the highest concentration tested. In contrast, ensovibep and MP0423, as single

molecules or as in combination, and the cocktail of two monoclonal antibodies remained effective and protected cells from CPE throughout the 4 passages.

While the application of ensovibep and MP0423 as single agents required higher concentrations, respectively 2 µg/mL and 10 µg/mL, after 4 passages, the combination of the two DARPin® antivirals retained effectiveness at a low concentration of 0.08 µg/mL. The mixture of the two monoclonal antibodies, REGN10933 & REGN10987, prevented the selection of escape mutants at a concentration of 0.4 µg/mL after passage 4.

Discussion

Novel emerging variants of the virus are an ever-present threat, as they may escape the antibodies generated during immunization or developed as therapeutics.

Here, we show that our two multi-specific DARPin® antivirals give high levels of protection against the currently most frequently reported SARS-CoV-2 mutations as well as two recently identified variants. Neutralization tests using VSV-based pseudoviruses carrying SARS-CoV-2 spike variants with nine mutations of the UK lineage B.1.1.7 and five mutations for the South African lineage B.1.351 showed inhibitory potencies for ensovibep that were comparable to that for the corresponding wild type form. While MP0423 was also highly active against the B.1.351 variant, a partial potency decrease was observed against the UK variant B.1.1.7, which is likely caused by a loss of binding on the S2 binding DARPin® domain. Of note, this lowered potency is still in therapeutically active potency range described by many monoclonal antibodies.

The analysis of all the most frequently occurring single-point mutations (i.e. A222V, K417E, N439K, S477N, E484K, N501Y, D614G) in pseudovirus-based neutralization tests resulted in no loss in potency for both DARPin® antivirals. In addition, we also evaluated less frequent single point-mutations (i.e. G446V, G476S, T478I, P479S, V483A, F486V, Q493K, F490S) within the epitope region of the three RBD binders of ensovibep[15] or mutations known to impact other therapeutics[10,19,20]. Among all tested single mutations, only F486V caused a strong decrease in potency for ensovibep, when compared to the wild-type. This finding is in line with our previous structural analysis[15]. Most importantly, F486 is also a critical residue for the virus itself, allowing binding to the ACE2 receptor and thus cell infection. Therefore, mutations of the phenylalanine at position 486 will decrease the affinity between the RBD and human ACE2 receptor and lower the infectivity of the virus[21,22]. To date, F486 is not present at high frequency in any circulating SARS-CoV-2 strain. In contrast to the loss of potency observed with the single RBD binders, one of which is in MP0423, mutation of F486V did not impact negatively on the neutralization capacity of MP0423. This highlights the value of the triple epitope binding mechanism of action of MP0423 – loss of binding of one of the domains is compensated for by the remaining two. This is also described in Suppl Fig 2.

Some mutations at positions that were not predicted as key interaction residues for the three distinct RBD binders (e.g. E484K or Q493K), led to a reduction of the potency in one or several of the RBD binders, while the tri-specific ensovibep molecules maintained the full neutralization capacity. This demonstrates that a tri-specific DARPin® design with cooperative binding permits high potency inhibition, even in the case of one DARPin® domain losing binding affinity. This cooperativity is an

exclusive feature of a tri-specific approach, highlighting a key advantage of the multi-specific DARPin® design over cocktails of antibodies.

The high level of protection against viral escape mutations by ensovibep and MP0423 was further demonstrated in a viral passaging experiment: the single monoclonal antibodies and the monovalent-DARPin® RBD-2 binder were rapidly overcome by escape mutants, whereas both multi-specific DARPin® antivirals, individually or in combination, maintained potency up to passage 4, to an extent comparable to one of the best monoclonal antibody cocktails with emergency use authorization (EUA) status. Deep sequencing of the viral spike gene in various pools is currently in progress and will provide further insight into the modes of action of the two DARPin® antivirals.

Encouraged by the high level of neutralization of the two multi-specific DARPin® antivirals against the mutations and new variants evaluated in this study, further characterizations of the impact of additional mutations, such as at position K417 observed in the Brazilian P.1 lineage (K417T) or newer South African variants (K417N), are in progress and will remain an ongoing topic for SARS-CoV-2 diagnostics, as well as for current therapeutics and vaccines against COVID-19

Acknowledgements

The authors thank Dr. Gert Zimmer for the gift of the recombinant VSV (Institute of Virology and Immunology (IVI), CH-3147 Mittelhäusern, Switzerland, Department of Infectious Diseases and Pathobiology, Vetsuisse Faculty, University of Bern, CH-3012 Bern, Switzerland). The expression plasmid for the SARS-CoV-2 spike protein was kindly provided by Dr. Giulia Torriani and Dr. Isabella Eckerle (Department of Medicine, University of Geneva, Switzerland).

SR & JM were supported by Swiss Federal Office for Civil Protection (Grants Nr. 353008564/Stm, 353008218/Stm, and 353008560/Stm to Olivier Engler and Stefan Kunz).

We would like to thank for the supply of the two 2019-nCoV strains: i) 2019-nCoV/IDF0372/2020 provided by the National Reference Centre for Respiratory Viruses hosted by Institute Pasteur (Paris, France) and headed by Dr. Sylvie van der Werf.

Funding

All studies were funded by Molecular Partners AG, Switzerland.

Author contributions

S.Ro.; M.W.; F.M.; J.M.; S.Ry.; A.B.; V.C.; P.A.; M.S; O.E.: conceptualized and designed experiments; S.Ro.; J.M.; S.Ry; H.M; N.L.; S.H.; A.B.; C.I.; A.C.; T.H.; A.N.; T.L.; S.M.: performed laboratory experiments; F.M.; C.R.; F.R.: performed computational work; S.Ro.; M.W.; F.M.; J.M.; S.Ry.; H.M.; N.L.; S.H.; A.B.; C.I.; A.C.; C.R.; F.R.; K.D.; S.L.; P.A.; M.S.; O.E.: drafted the manuscript; S.L.; D.S; P.A.; M.S.: acquired funding; All authors reviewed the manuscript.

Competing interests: Molecular Partners authors own performance share units and/or stock of the company.

Figures

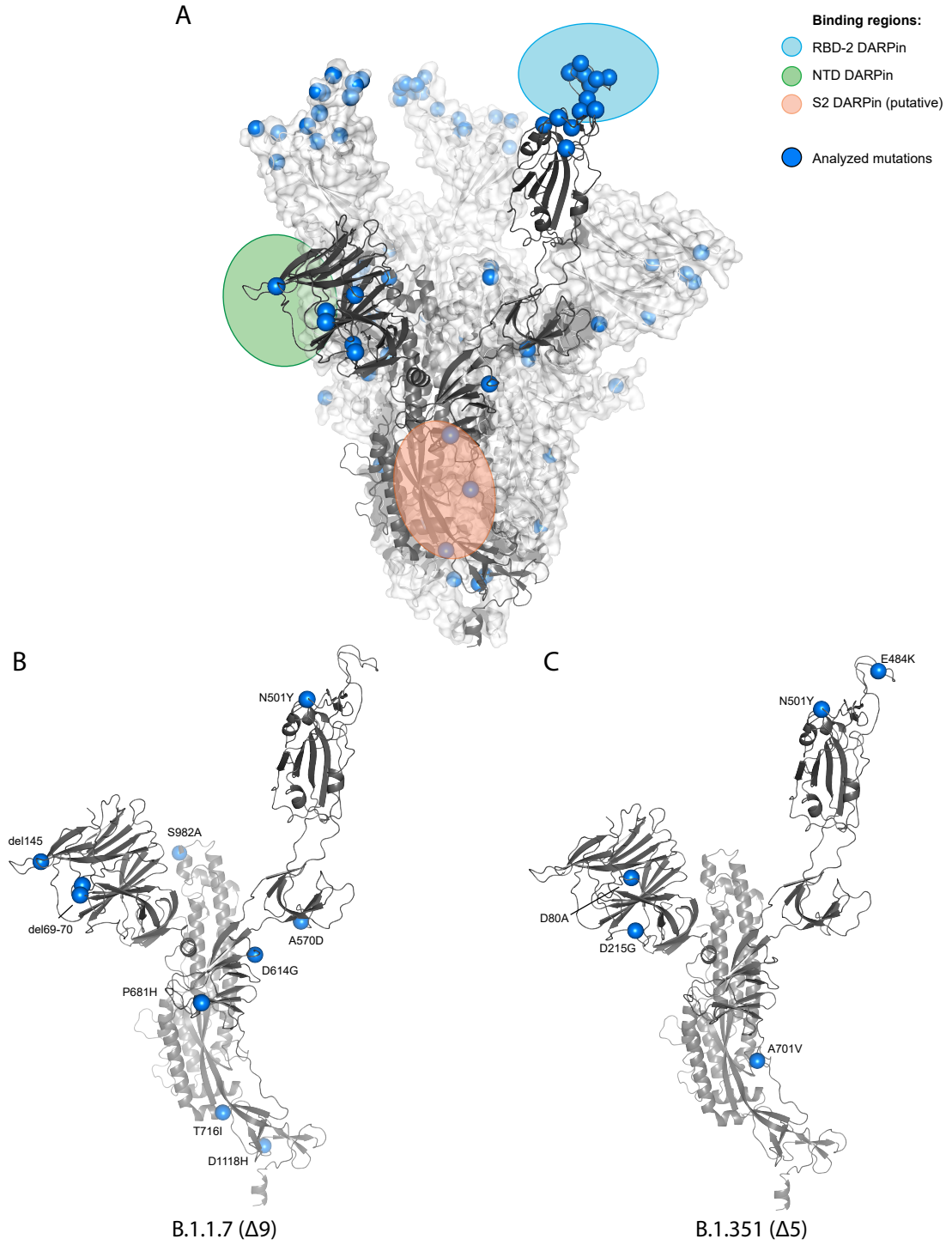

Figure 1: Structural visualization of critical mutations of the SARS-CoV-2 spike protein evaluated in this study. A) Representation of the full trimeric SARS-CoV-2 spike protein with all residues analyzed in the pseudovirus neutralization assay visualized as blue spheres. Binding regions for the individual DARPin® domains incorporated in ensovibep and MP0423 are colored in blue (RBD), green (NTD) and red (S2); B) Monomeric spike protein structure representing the variant first identified in the UK B.1.1.7 (del69-70, del145, N501Y, A570D, D614G, P681H, T716I, S982A, D1118H); C) Monomeric spike protein structure representing the variant first identified in the South Africa B.1.351 (D80A, D215G, E484K, N501Y, A701V). The PDB file 6xcn was used for generating the figures with PyMol version 2.1.1 (Schrödinger, LLC). In order to visualize all mutations, loops 518-520, 676-689, 811-813 and regions of the NTD domain missing in the cryo-EM structure, were modelled with MODELLER included in the BIOVIA Discovery Studio software using the PDB file 6zge as template for the NTD domain (BIOVIA, Dassault Systèmes, BIOVIA Discovery Studio 2021).

A

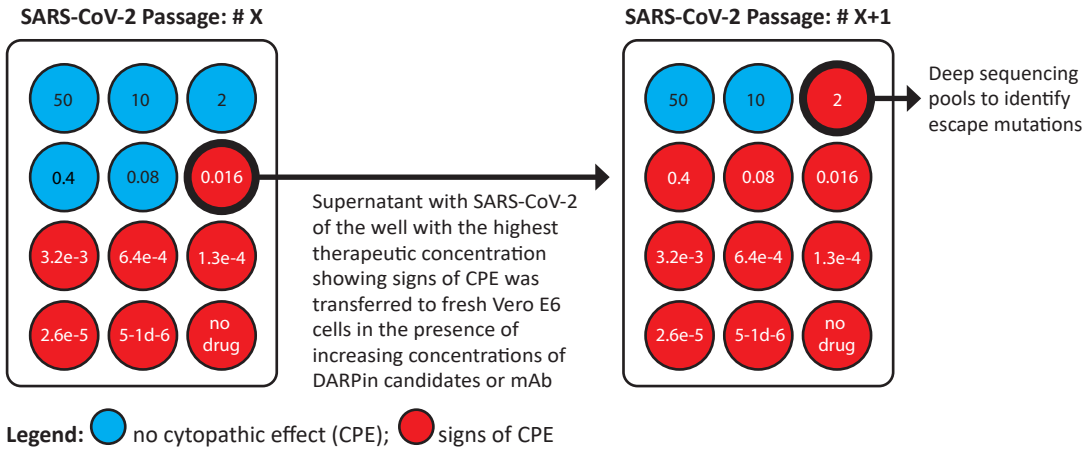

B

Passage #1	DARPin or Antibody Concentrations [µg/mL]						
Constructs	50	10	2	0.4	0.08	0.02	no drug
DARPin Candidates	Cytopathic Effect [%]						
RBD - 2	0%	0%	0%	5%	≥90%	≥90%	≥90%
ensovibep	0%	0%	0%	0%	≥90%	≥90%	≥90%
MP0423	0%	0%	0%	0%	≥90%	≥90%	≥90%
MP0420 & MP0423	0%	0%	0%	0%	≥90%	≥90%	≥90%
Antibody Candidates	Cytopathic Effect [%]						
S309	0%	0%	60%	≥90%	≥90%	≥90%	≥90%
REGN10933	0%	0%	0%	5%	80%	≥90%	≥90%
REGN10987	80%	≥90%	≥90%	≥90%	≥90%	≥90%	≥90%
REGN10933 & REGN10987	0%	0%	0%	0%	≥90%	≥90%	≥90%
IgG Negative Control	≥90%	≥90%	≥90%	≥90%	≥90%	≥90%	≥90%

Passage #2	DARPin or Antibody Concentrations [µg/mL]						
Constructs	50	10	2	0.4	0.08	0.02	no drug
DARPin Candidates	Cytopathic Effect [%]						
RBD - 2	0%	60%	≥90%	≥90%	≥90%	≥90%	≥90%
ensovibep	0%	0%	0%	0%	0%	50%	≥90%
MP0423	0%	0%	0%	0%	0%	≥90%	≥90%
MP0420 & MP0423	0%	0%	0%	0%	0%	≥90%	≥90%
Antibodies Candidates	Cytopathic Effect [%]						
S309	≥90%	≥90%	≥90%	≥90%	≥90%	≥90%	≥90%
REGN10933	0%	0%	80%	≥90%	≥90%	≥90%	≥90%
REGN10987	≥90%	≥90%	≥90%	≥90%	≥90%	≥90%	≥90%
REGN10933 & REGN10987	0%	0%	0%	0%	0%	≥90%	≥90%
IgG Negative Control	≥90%	≥90%	≥90%	≥90%	≥90%	≥90%	≥90%

Passage #3	DARPin or Antibody Concentrations [µg/mL]						
Constructs	50	10	2	0.4	0.08	0.02	no drug
DARPin Candidates	Cytopathic Effect [%]						
RBD - 2	≥90%	≥90%	≥90%	≥90%	≥90%	≥90%	≥90%
ensovibep	0%	0%	0%	0%	≥90%	≥90%	≥90%
MP0423	0%	0%	0%	40%	≥90%	≥90%	≥90%
MP0420 & MP0423	0%	0%	0%	0%	≥90%	≥90%	≥90%
Antibodies Candidates	Cytopathic Effect [%]						
S309	≥90%	≥90%	≥90%	≥90%	≥90%	≥90%	≥90%
REGN10933	0%	0%	5%	≥90%	≥90%	≥90%	≥90%
REGN10987	≥90%	≥90%	≥90%	≥90%	≥90%	≥90%	≥90%
REGN10933 & REGN10987	0%	0%	0%	0%	≥90%	≥90%	≥90%
IgG Negative Control	≥90%	≥90%	≥90%	≥90%	≥90%	≥90%	≥90%

Passage #4	DARPin or Antibody Concentrations [µg/mL]						
Constructs	50	10	2	0.4	0.08	0.02	no drug
DARPin Candidates	Cytopathic Effect [%]						
RBD - 2	n.d.	n.d.	n.d.	n.d.	n.d.	n.d.	n.d.
ensovibep	0%	0%	0%	40%	≥90%	≥90%	≥90%
MP0423	0%	0%	≥90%	≥90%	≥90%	≥90%	≥90%
MP0420 & MP0423	0%	0%	0%	0%	5%	≥90%	≥90%
Antibodies Candidates	Cytopathic Effect [%]						
S309	n.d.	n.d.	n.d.	n.d.	n.d.	n.d.	n.d.
REGN10933	≥90%	≥90%	≥90%	≥90%	≥90%	≥90%	≥90%
REGN10987	n.d.	n.d.	n.d.	n.d.	n.d.	n.d.	n.d.
REGN10933 & REGN10987	0%	0%	0%	0%	≥90%	≥90%	≥90%
IgG Negative Control	n.d.	n.d.	n.d.	n.d.	n.d.	n.d.	n.d.

Figure 2: Ensovibep and MP0423 protect from viral escape mutants*:* A) Schematic representation of the procedure: French SARS-CoV-2 isolate from early 2020 (1.5 x10^6 pfu) was incubated in presence of increasing concentrations of DARPin® or antibody for 4 days on Vero E6 cells and virus-induced cytopathic effects (CPE) were determined by microscopy. For each DARPin® and antibody condition, cultures showing significant cytopathic effect (≥20%) under the greatest selective pressure were selected and virus-containing supernatant collected to start a new culture passage on Vero E6 cells, again under increasing concentrations of the corresponding DARPin® or monoclonal antibody condition. Passaging of virus containing supernatant was continued in the same manner for a total of 4 passages. B) Tabular representation of the cytopathic effects induced by SARS-CoV-2 cultured in presence of increasing concentrations of mono-valent DARPin® binder RBD-2, multi-specific DARPin® antivirals ensovibep and MP0423 or a cocktail of ensovibep and MP0423 and the antibody antivirals S309, REGN10933 and REGN10987 or a cocktail of REGN10933 and REGN10987 through passage 1 to 4. A cytopathic effect (CPE) judged by microscopy to be less than 20% is colored in blue and a CPE estimated ≥20% is colored in red. Indicated with a dark border are the culture supernatants chosen for further passaging under selective pressure and for deep sequencing (data in process).

Tables

Table 1a: Summary of the neutralizing efficacy of multi-specific DARPin®s and monoclonal antibodies against VSV-SARS-CoV-2 pseudoviruses carrying spike variants. The spike variants and mutations were incorporated into VSV-pseudoviruses encoding luciferase as reporter gene. Neutralization tests for multi-specific DARPin®s, ensovibep and MP0423 and two neutralizing antibodies, REGN10933 and REGN10987, were performed and IC_{50} (ng/mL) values are shown for each experimental condition.

Variants	Rational	VSV Pseudotype Neutralization Assay IC_{50} [ng/mL]			
		Ensovibep	MP0423	REGN10933	REGN10987
wild type	(Wuhan)	1.0	3.1	3.9	6.1
B.1.351	(SA, Δ5)*	3.0	2.4	19	6.2
B.1.1.7	(UK, Δ9)**	1.7	70	2.4	3.5
Individual Mutations	Residues in variants				
N501Y	in UK, SA, BRA variants; increases RBD/ACE2 interaction[1]	0.5	1.4	4.3	5.8
E484K	in SA, BRA variants; increases RBD/ACE2 interaction[1]	2.7	1.8	17	5.8
K417E	residue mutated to N/T in SA, BRA variants	0.5	1.2	>100	1.5
Y453F	key residue evolved in Danish mink farms variants	3.2	2.0	>100	12
Individual Mutations	Highly frequent mutations				
D614G	Wide global spread	2.4	2.8	n.d.	n.d.
S477N	Wide global spread	1.9	0.8	n.d.	n.d.
N439K	Wide spread in northern amerika, UK; increases RBD/ACE2 interaction[1]	1.3	2.5	2.8	30
A222V	Wide European spread	2.2	3.1	7.0	2.9
Individual Mutations	Within RBD epitope of DARPin®s or reported resistance mutation for other therapeutics				
G446V		1.7	1.0	1.5	>100
G476S		1.5	3.1	n.d.	n.d.
T478I		2.7	2.8	4.0	7.0
P479S		2.1	1.5	3.7	9.8
V483A		2.3	1.9	n.d.	n.d.
F486V	key residue for DARPin® RBD binder[2]; reduces RBD/ACE2 interaction[1]	>100	7.7	>100	4.4
Q493K		7.9	2.4	>100	10
F490S	Reduces RBD/ACE2 interaction[1]	3.8	1.6	3.1	9.2

n.d.: not determined
**Mutations (SA): D80A, D215G, E484K, N501Y, A701V*
***Mutations (UK): del69-70, del145, N501Y, A570D, D614G, P681H, T716I, S982A, D1118H*
Blue shade: no or marginal loss in neutralization potency by therapeutics
Yellow shade: IC50 values between 10-100 ng/mL (in a therapeutically active range)
Red shade: IC50 values between >100 ng/mL (outside therapeutically active range)
[1] Influence of residue mutations on spike protein binding to human ACE2 (Yi et al. 2020)
[2] Predicted interaction residue for DARPin® RBD binder (Walser et al. 2020)

Table 1b: Summary of the neutralizing efficacy of multi-specific DARPin® ensovibep and its mono-valent RBD-binding DARPin® domains against VSV-SARS-CoV-2 pseudoviruses carrying spike variants. The spike variants and mutations were incorporated into VSV-pseudoviruses encoding luciferase as reporter gene. Neutralization tests for multi-specific DARPin® ensovibep as well as the mono-valent DARPin® domains RBD-1, RBD-1, RBD-3 were performed and IC_{50} (ng/mL) values are shown for each condition.

Variants	Rational	VSV Pseudotype Neutralization Assay IC_{50} [ng/mL]			
		Ensovibep	Mono-valent RBD Binders in MP0420		
			RBD-1	RBD-2	RBD-3
wild type	(Wuhan)	1.0	7.2	2.1	13.3
B.1.351	(SA, Δ5)*	3.0	**76**	**26**	**>100**
B.1.1.7	(UK, Δ9)**	1.7	4.6	5.4	11.7
Individual Mutations	Residues in variants				
N501Y	in UK, SA, BRA variants; increases RBD/ACE2 interaction[1]	0.5	9.1	4.8	27.8
E484K	in SA, BRA variants; increases RBD/ACE2 interaction[1]	2.7	**64.2**	10.2	**>100**
K417E	residue mutated to N/T in SA, BRA variants	0.5	1.8	1.0	3.6
Y453F	key residue evolved in Danish mink farms variants	3.2	10.9	5.9	3.3
Individual Mutations	Highly frequent mutations				
D614G	Wide global spread	2.4	11.9	6.2	23
S477N	Wide global spread	1.9	3.0	2.0	9.0
N439K	Wide spread in northern amerika, UK; increases RBD/ACE2 interaction[1]	1.3	7.3	5.3	12.9
A222V	Wide European spread	2.2	3.3	4.6	19.5
Individual Mutations	Within RBD epitope of DARPin®s or reported resistance mutation for other therapeutics				
G446V		1.7	0.7	1.8	2.3
G476S		1.5	2.3	3.7	29
T478I		2.7	11.2	3.1	16.7
P479S		2.1	7.2	2.3	27.6
V483A		2.3	21.8	8.4	21.3
F486V	key residue for DARPin® RBD binder[2]; reduces RBD/ACE2 interaction[1]	>100	**>100**	**>100**	**>100**
Q493K		7.9	30	**28.2**	45.8
F490S	Reduces RBD/ACE2 interaction[1]	3.8	2.3	1.7	8.1

n.d.: not determined

**Mutations (SA): D80A, D215G, E484K, N501Y, A701V*

***Mutations (UK): del69-70, del145, N501Y, A570D, D614G, P681H, T716I, S982A, D1118H*

Blue shade: no or marginal loss in neutralization potency by therapeutics

Red shade: IC50 values between >100 ng/mL (outside therapeutically active range)

Bold font >5-fold loss in IC_{50} of mono-valent RBD binders (compared to wild type)

[1] Influence of residue mutations on spike protein binding to human ACE2 (Yi et al. 2020)

[2] Predicted interaction residue for DARPin® RBD binder (Walser et al. 2020)

Supplementary Materials for

Multi-specific DARPin® therapeutics demonstrate very high potency against mutated SARS-CoV-2 variants

Rothenberger et al. 2021

Materials and Methods

Generation of His-tagged mono-valent RBD binders, ensovibep, MP0423 and the domain k.o. variants of MP0423

DARPin® construct selected and cloned as described in Walser et al.[15] was transformed in *E.coli* BL21 cells, plated on LB-agar (containing 1% glucose and 50 µg/ml ampicillin) and then incubated overnight at 37°C. Single colony was picked into TB medium (containing 1% glucose and 50 µg/ml ampicillin) and incubated overnight at 37°C, shaking at 230 rpm. Fresh TB medium (containing 50 µg/ml ampicillin) was inoculated with 1:20 of overnight culture and incubated at 37°C at 230 rpm. At OD600 = 1.1 the culture was induced by addition of IPTG (0.5mM final concentration) and incubated for further 5h at 37°C and 230 rpm. Harvest was done by centrifugation (10 min 5000 x g). After cell disruption by sonication, primary recovery was done by heat treatment for 30 min at 62.5°C and subsequent centrifugation (15 min, 12000 x g). 20mM Imidazole and 1% Triton X-100 was added to the supernatant and the 0.22µm filtered supernatant was further purified by immobilized metal affinity chromatography (HisTrap FF crude, Cytiva, Sweden) using the N-terminal His-tag including a wash step with 1% Triton X-100 and a step elution with 250 mM Imidazole. In a subsequent step, the elution fraction of the IMAC step is applied on a size exclusion chromatography (Superdex 200, Cytiva, Sweden) and fractions of interest are pooled and concentrated. Finally, the concentrated sample was filtered through a 0.22 µm Mustang E filter for Endotoxin removal and sterile filtration and quality controlled.

Generation of monoclonal antibodies, REGN10933, REGN10987 and S309

Publicly available sequences of variable domains from monoclonal antibodies RGN10933, RGN10987 (WHO Drug Information, Vol. 34, No. 3, 2020, Proposed INN: List 124 – COVID-19) and S309 (PDB: 6WPS) were used to synthetize the corresponding cDNA fragments and cloned into a proprietary expression vector at Evitria AG (Switzerland). Generated vectors containing the constant immunoglobulin hIgG1 chain or kappa light chain were used for transfection in Chinese hamster ovary cells by Evitria. Sterile filtered cell supernatants were purified via affinity purification with HiTrap MabSelect column followed by a size exclusion chromatography using HiLoad 26/600 Superdex 200 column in PBS pH7.4. Selected fractions were pooled and quality controlled (by SDS-PAGE, size exclusion chromatography and endotoxin measurement), before use in assays.

VSV-SARS-CoV-2 pseudotype mutation-vector generation

Plasmid pCAGGS containing the spike protein of SARS-CoV-2[15] was used as template for generation of single and multiple spike protein mutants. Forward and reverse complementary primers encoding the

mutation were synthesized by Microsynth (Balgach, Switzerland). High-fidelity Phusion polymerase (New England Biolabs, USA) was used for all DNA amplification.

Single mutations of the spike protein were generated via two PCR fragments of the spike ORF using high-fidelity Phusion polymerase (New England Biolabs, USA). The first fragment was generated via a generic forward primer (pCAGGS-5) annealing upstream of the spike ORF and the specific reverse primer encoding the mutation. The second fragment was generated using the specific forward primer encoding the mutation and a reverse primer (rbglobpA-R). The two fragments were gel-purified and used as input for an assembly PCR without addition of flanking primers.

For multi-mutation spike proteins, a complementary pair of primers (forward and reverse) encoding each mutation was designed. Fragment 1 was generated with forward primer pCAGGS-5 and reverse primer encoding mutation 1. Fragment 2 was generated using forward primer encoding mutation 1 and reverse primer encoding mutation 2. All subsequent fragments were generated analogously. DNA fragments were gel-purified and mixed in equimolar amounts. This mix was used for re-assembly of the full spike ORF using outer primers pCAGGS-5 and rbglobpA-R.

For both single as well as multi-mutation spike protein, the full-length spike ORF was isolated from an agarose gel, digested by restriction enzymes NheI/EcoRI and inserted into the pCAGGS vector backbone. The correct sequence was verified via sequencing the whole ORF of the spike protein by Microsynth (Balgach, Switzerland).

VSV-SARS-CoV-2 pseudotype neutralization assay for mutational analysis and MP0423 domain knock outs

The pseudotype viral system was based on the recombinant VSV*ΔG-Luc vector in which the glycoprotein gene (G) had been deleted and replaced with genes encoding green fluorescent protein and luciferase[23]. Pseudoviruses were generated as reported previously[24,25]. For the neutralization assay, an initial dilution of the compounds was followed by three-fold dilutions in quadruplicates in DMEM-2 % [vol/vol] FCS supplemented with 20 µM human serum albumin (CSL Behring). The mixture was mixed with an equal volume of DMEM-2 % FCS containing 250 infectious units (IU) per well of SARS-CoV-2 pseudoviruses and incubated for 90 min at 37°C. The mix was inoculated onto Vero E6 cells in a clear bottom white walled 96-well plate during 90 min at 37°C. The inoculum was removed and fresh medium added, and cells further incubated at 37°C for 16 h. Cell were lysed according to the ONE-Glo™ luciferase assay system (Promega, Madison, US) and light emission was recorded using a Berthold® TriStar LB941 luminometer. The raw data (relative light unit values) were exported to GraphPad Prism v8.4.3, and the % neutralization values were normalized to the untreated PsV signal. IC_{50} with 95% confidence interval were estimated by model of nonlinear regression fit with settings for log (inhibitor) vs normalized response curves. Data points are plotted by the mean ±SEM (standard error of mean).

Cells and pathogenic virus

Vero E6 cells (kindly provided by Prof. Volker Thiel, University of Bern, Switzerland) were passaged in Minimum Essential Medium (MEM) (Cat N° M3303) containing 10% fetal bovine serum (FBS) and supplements (2 mM L-Glutamine, 1% Non-essential amino acids, 100 U/ml Penicillin, 100 µg/ml Streptomycin, 0.06% Sodium bicarbonate, all from Bioswisstec, Schaffhausen, Switzerland) at 37°C, >85% humidity and 5% CO_2. SARS-CoV-2 (2019-nCoV/IDF0372/2020), kindly provided by Dr. Sylvie van der Werf from the National Reference Centre for Respiratory Viruses hosted by Institut Pasteur (Paris, France) was propagated in Vero E6 cells in MEM containing 2% FBS and supplements (2%-FBS-MEM) at 37°C, >85% humidity and 5% CO_2. Viral titer was determined by standard plaque, by incubating 10-fold serial dilutions of the virus for 1h at 37°C on a confluent 24-well plate with Vero E6 cells. Then inoculum was removed and 1 ml overlay medium (20 ml Dulbecco's Modified Eagle's Medium, 5 ml FBS, 100 U/ml Penicillin, 100 µg/ml Streptomycin, and 25 ml Avicel rc581) was added. After 3 days incubation at 37°C the overlay was removed and the plates stained with crystal violet solution (spatula tip (~4 mg) crystal violet powder (Sigma Aldrich) solved in 30 ml 37% formalin and 120 ml PBS (Sigma Aldrich).

Viral passaging experiment with authentic SARS-CoV-2

Virus escape studies were adapted from a previously published protocol by Baum et al.[10]. Briefly, 1:5 serial dilutions of DARPin® antivirals and monoclonal antibodies from 100 µg/mL to 0.032 µg/mL were prepared in Minimum Essential Medium (MEM) containing 2% FBS, supplements and 10 µM human serum albumin (HSA; CSL Behring, Switzerland; 2%-FBS-MEM + HSA). 500 ul of virus suspension containing 1.5 x 10^6 plaque forming units (pfu) SARS-CoV-2 in 2%-FBS-MEM + HSA were mixed with 500 µl of serially diluted DARPin® molecules or monoclonal antibodies and subsequently incubated for 1 hour at 37°C. The mixtures were then transferred to confluent Vero E6 cells in 12 well plates and incubated for 4 days at 37°C, >85% humidity and 5% CO_2. Each culture well was assessed for cytopathic effect (CPE) by microscopy. Supernatant was removed from wells with the highest DARPin® or antibody concentrations showing significant CPE (≥20%) and used for total RNA extraction and further passaging. For subsequent rounds of passaging, remaining 900 µl supernatant of selected wells was diluted to 4 ml in 2%-FCS-MEM + HSA and thereof 500 µl mixed with serial dilutions of DARPin® molecules or antibodies, incubated and the mixture transferred to 12-well plates with fresh Vero E6 cells as described above. Cell culture wells were assessed for CPE again after 4 days and the supernatant of wells with highest DARPin® or antibody concentrations with evident viral replication (CPE) harvested and used for additional passages. A total of 4 passages were performed this way.

Virus neutralization of authentic SARS-CoV-2 determined by Cell Titer-Glo and real-time RT-PCR

Virus neutralization capacity of mono-valent DARPin® candidate and multi-specific DARPin® molecules was determined for 100 $TCID_{50}$ SARS-CoV-2 by measuring ATP levels of protected cells in a cell viability assay. DARPin® molecules were serially diluted 1:4 from 40 nM to 2.4 pM (in triplicates) in 100 µl cell culture medium (2%-FBS-MEM) enriched with 10 µM HSA in 96 well plates. The diluted DARPin® antivirals were mixed with 100 $TCID_{50}$ SARS-CoV-2 in 100 µl 2%-FBS-MEM + HSA and incubated for 1 h at 37°C. DARPin®/virus mixtures (200 µl) were transferred onto confluent Vero E6 cells. The controls consisted of Vero E6 cells exposed to virus suspension only, to determine maximal cytopathic effect and of cells incubated with medium only, to determine baseline state of cells. The plates were incubated for 3 days at 37°C, >85% humidity and 5% CO_2. Cell viability was determined by removing 100 µl supernatant from all wells and adding 100 µl CellTiter-Glo reagent as described in the manufacturers protocol (CellTiter-Glo® Luminescent Cell Viability Assay, Promega, Madison, USA). Luminescence was read after 2 minutes shaking on an orbital shaker, transferring the mixture to an opaque-walled plate and 10 min incubation at room temperature using the GloMax instrument (Promega). To determine inhibition of virus replication, the previously removed supernatant (100 µl) was inactivated in 400 µl AVL-buffer (Qiagen, Hilden, Germany) and 400 µl 100% ethanol and extracted and eluted in 100 µl using the MagNAPure 96 system (Roche, Basel, Switzerland). Viral RNA was quantified by real-time RT-PCR targeting the E gene (Eurosurveillance | Detection of 2019 novel coronavirus (2019-nCoV) by real-time RT-PCR) using 5 µl RNA and 20 µl TaqMan Fast Virus 1-Step Master Mix (Life Technologies, Zug, Switzerland). Viral genome equivalents (ge) were calculated using a regression analysis and an internal standard.

Supplementary Figures

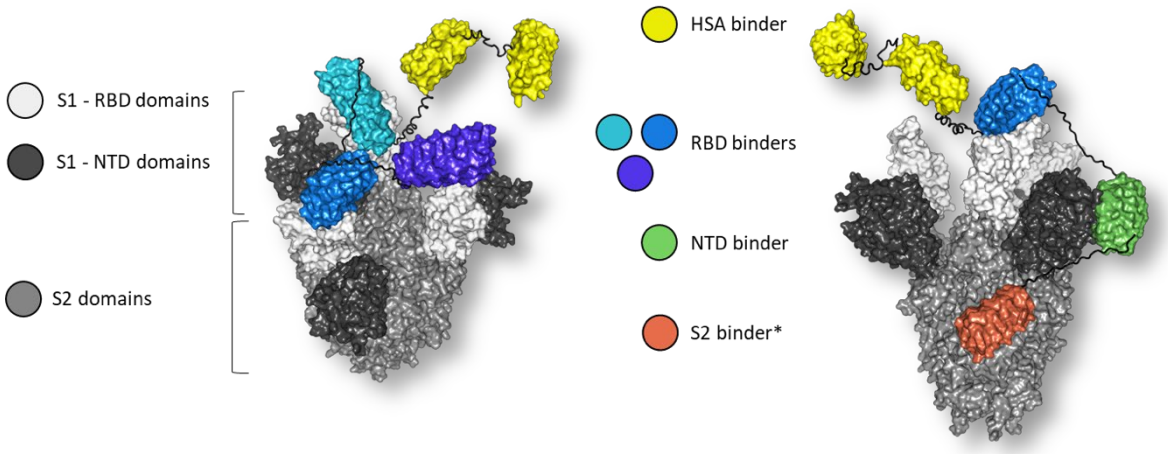

Supplementary Figure 1: Molecular model of multi-specific DARPin® antivirals MP0423 (right), consisting of five DARPin® domains (yellow: HSA-binding domains, blue: RBD-binding domain, green: NTD-binding domain, orange: S2-binding domain) bound to the spike ectodomain. Linkers are shown in black. Molecular model of multi-paratopic DARPin® candidate ensovibep (left) consisting of five DARPin® domains (yellow: HSA-binding domains, shades of blue: RBD-binding domains) bound to the RBDs (white) of the spike ectodomain (grey). Linkers are shown in black. Position of RBD and NTD binders guided by Cryo-EM data. *Positioning on spike protein remains uncertain for the S2 binder and is guided by manual docking and not based on Cryo-EM data[15].

A

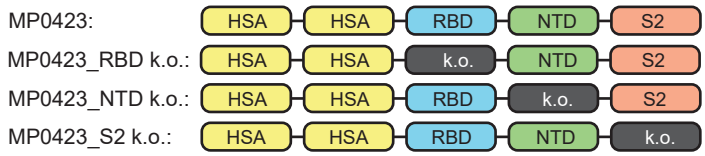

B

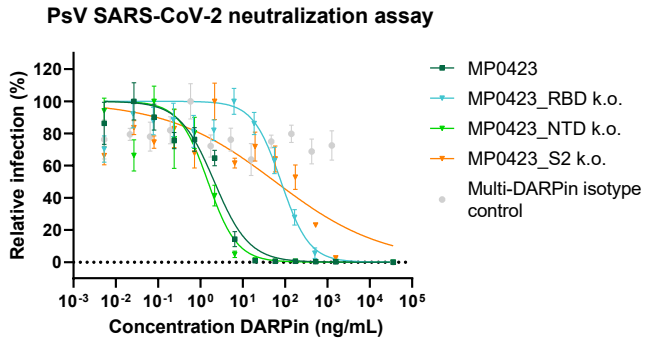

C

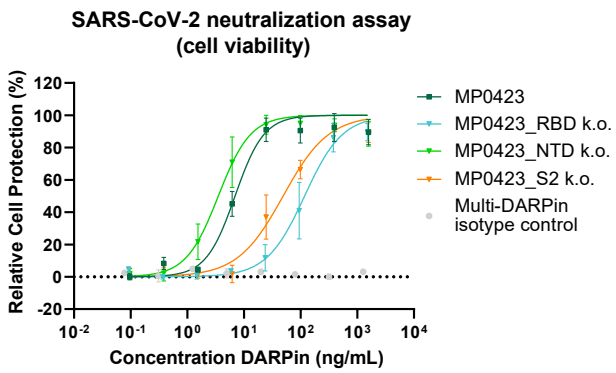

D

	ng/mL		
	IC_{50} (PsV)	EC_{50} (cell viability)	IC_{50} (RT-qPCR)
MP0423	2.1	7	3.2
MP0423_RBD k.o.	80.5	117.5	20.8
MP0423_NTD k.o.	1.5	3.5	1.8
MP0423_S2 k.o.	58.8	49.1	28.8

Neutralization potency:

MP0423 ~ MP0423_NTD k.o. > MP0423_RBD k.o. ~ MP0423_S2 k.o.

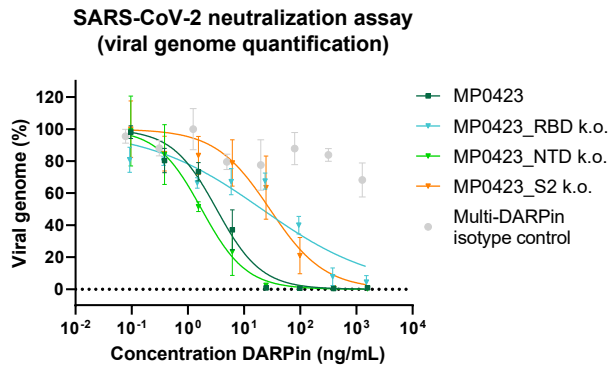

Supplementary Figure 2: Determination of the contribution of the single DARPin® domains of MP0423 in the neutralization activity against SARS-CoV-2. A) Schematic representation of the multi-specific MP0423 knock-out (k.o) constructs. In each k.o. construct, the indicated SARS-CoV-2-binding domain is replaced by a non-binding DARPin®. HSA: HSA-binding DARPin®, RBD: RBD-binding DARPin®, NTD: NTD-binding DARPin®, S2: S2-binding DARPin®; **B)** Neutralization profiles of MP0423 and k.o constructs against VSV-SARS-CoV-2 pseudoviruses expressing the wild-type spike protein; **C)** Upper panel: protective effect of DARPin® molecules against SARS-CoV-2 (100 pfu)-mediated cytopathic effect. Depicted are the percentage of cell protection conferred by MP0423 or the k.o contructs. Cell protection was determined after 3 days of incubation by measuring intracellular ATP levels in a cell viability assay using Cell Titer-Glo. Lower panel: inhibition of SARS-CoV-2 viral replication quantified by real-time RT-PCR and expressed as percentage of viral genome equivalents present in the supernatant of Vero E6 cells exposed to 100 pfu SARS-CoV-2 with increasing amounts of MP0423 or k.o. constructs. **D)** IC_{50}/EC_{50}values and potency ranking of the constructs analyzed. No potency loss compared to MP0423 was observed for MP0423_NTD k.o. while a reduction in neutralization activity was observed for the MP0423_RBD k.o. and the MP0423_S2 k.o. constructs.

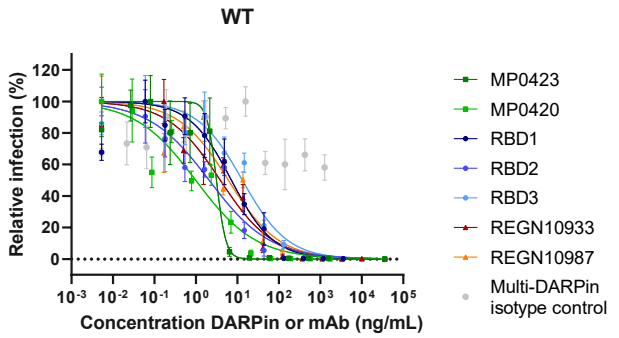
WT
Relative infection (%)
Concentration DARPin or mAb (ng/mL)
MP0423
MP0420
RBD1
RBD2
RBD3
REGN10933
REGN10987
Multi-DARPin isotype control

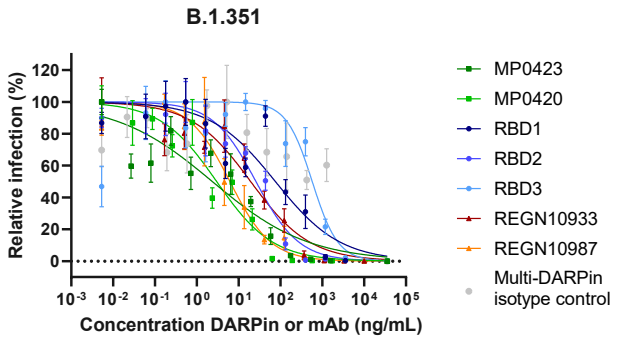
B.1.351
Relative infection (%)
Concentration DARPin or mAb (ng/mL)
MP0423
MP0420
RBD1
RBD2
RBD3
REGN10933
REGN10987
Multi-DARPin isotype control

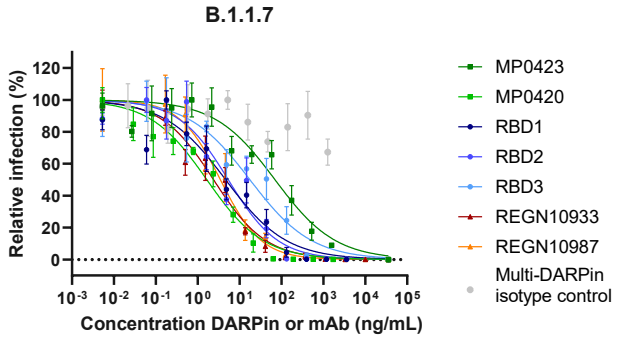
B.1.1.7
Relative infection (%)
Concentration DARPin or mAb (ng/mL)
MP0423
MP0420
RBD1
RBD2
RBD3
REGN10933
REGN10987
Multi-DARPin isotype control

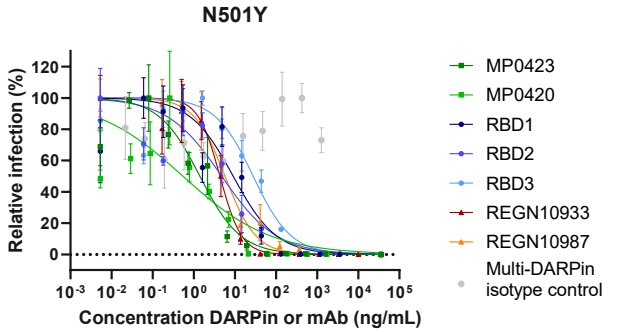
N501Y
Relative infection (%)
Concentration DARPin or mAb (ng/mL)
MP0423
MP0420
RBD1
RBD2
RBD3
REGN10933
REGN10987
Multi-DARPin isotype control

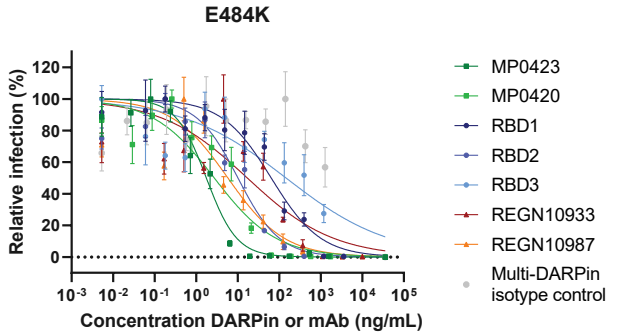
E484K
Relative infection (%)
Concentration DARPin or mAb (ng/mL)
MP0423
MP0420
RBD1
RBD2
RBD3
REGN10933
REGN10987
Multi-DARPin isotype control

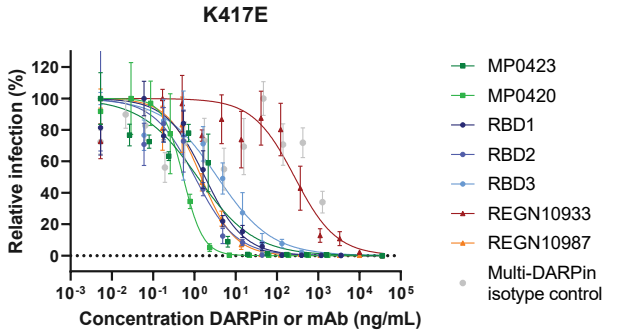
K417E
Relative infection (%)
Concentration DARPin or mAb (ng/mL)
MP0423
MP0420
RBD1
RBD2
RBD3
REGN10933
REGN10987
Multi-DARPin isotype control

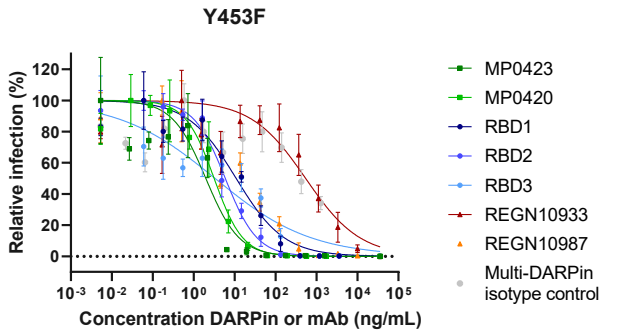
Y453F
Relative infection (%)
Concentration DARPin or mAb (ng/mL)
MP0423
MP0420
RBD1
RBD2
RBD3
REGN10933
REGN10987
Multi-DARPin isotype control

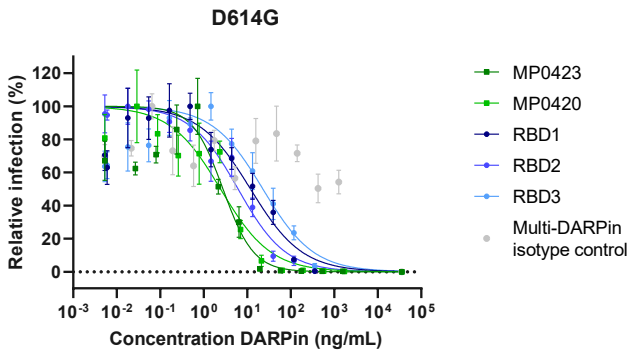
D614G
Relative infection (%)
Concentration DARPin (ng/mL)
MP0423
MP0420
RBD1
RBD2
RBD3
Multi-DARPin isotype control

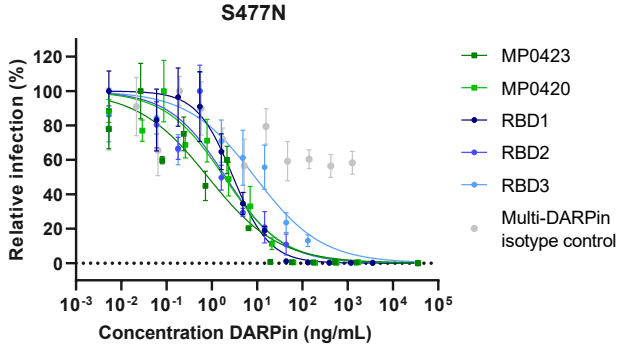
S477N
Relative infection (%)
Concentration DARPin (ng/mL)
MP0423
MP0420
RBD1
RBD2
RBD3
Multi-DARPin isotype control

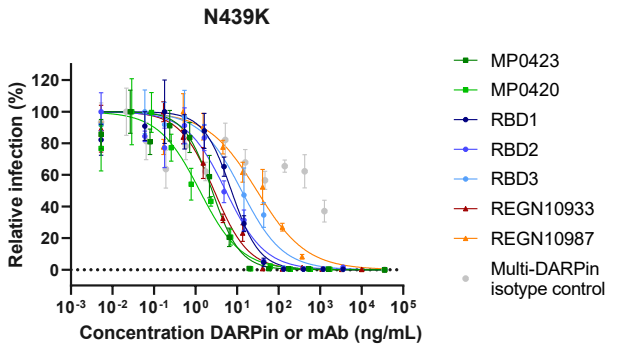
N439K
Relative infection (%)
Concentration DARPin or mAb (ng/mL)
MP0423
MP0420
RBD1
RBD2
RBD3
REGN10933
REGN10987
Multi-DARPin isotype control

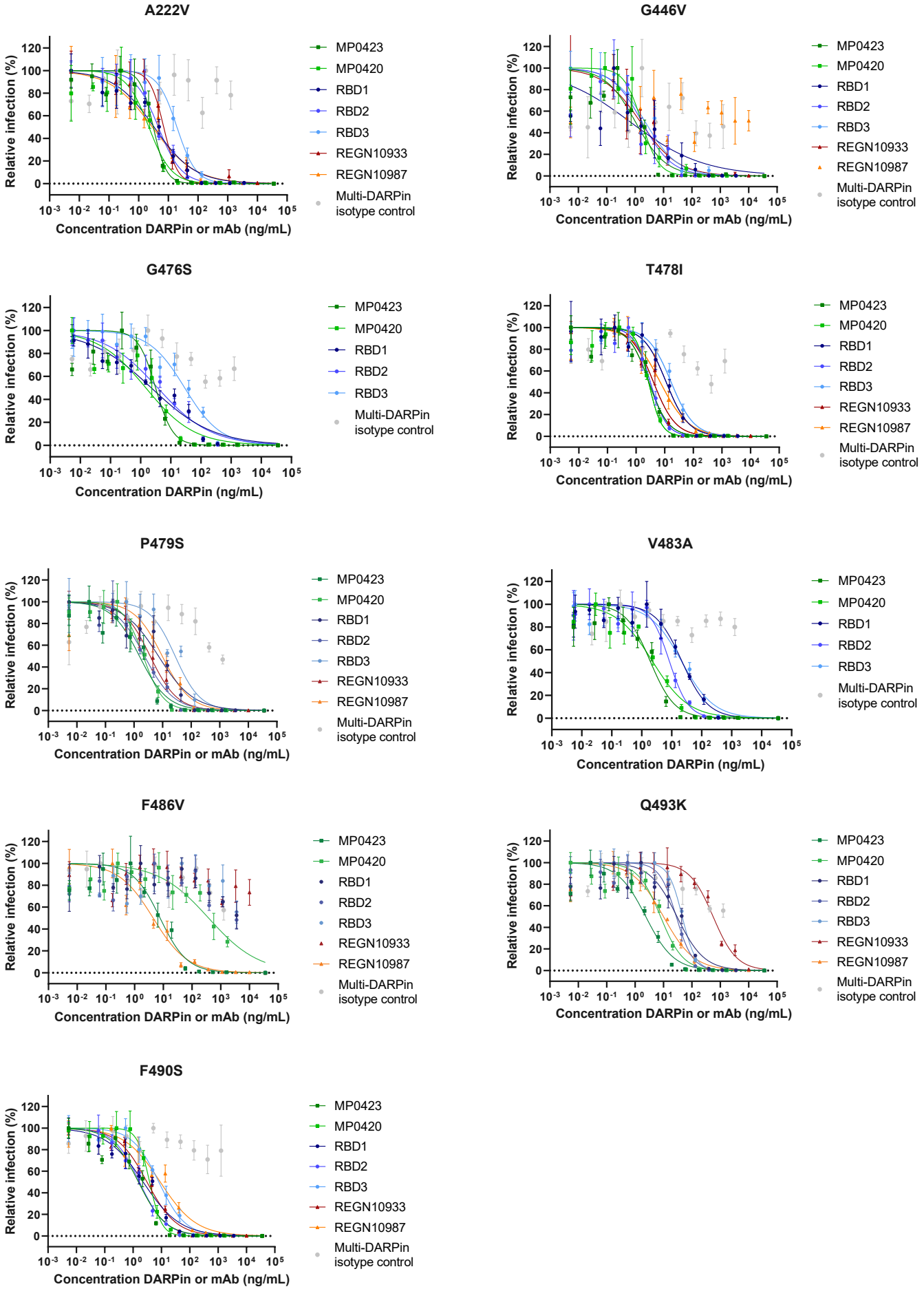

Supplementary Figure 3: Titration curves for ensovibep (MP0420) and its RBD-binding domains (i.e. RBD-1, RBD-2 and RBD-3), MP0423, REGN10933 and REGN10987 to determine IC_{50} neutralization potencies on various VSV-SARS-CoV-2 mutants and variants summarized in Table 1.

References

1 Andreano, E. *et al.* SARS-CoV-2 escape in vitro from a highly neutralizing COVID-19 convalescent plasma. *bioRxiv*, doi:10.1101/2020.12.28.424451 (2020).

2 Voloch, C. M. *et al.* Novel circulating lineage of SARS-CoV-2 in the state of Rio de Janeiro Brazil originated from B.1.1.28 lineage. *medRxiv*, doi:10.1101/2020.12.23.20248598 (2020).

3 Thomson, E. C. *et al.* The circulating SARS-CoV-2 spike variant N439K maintains fitness while evading antibody-mediated immunity. *bioRxiv*, doi:10.1101/2020.11.04.355842 (2020).

4 Wang, P. *et al.* Increased Resistance of SARS-CoV-2 Variants B.1.351 and B.1.1.7 to Antibody Neutralization. *bioRxiv*, doi:10.1101/2021.01.25.428137 (2021).

5 Kupferschmidt, K. Fast-spreading U.K. virus variant raises alarms. *Science* 371, 9-10, doi:10.1126/science.371.6524.9 (2021).

6 Tegally, H. *et al.* Emergence and rapid spread of a new severe acute respiratory syndrome-related coronavirus 2 (SARS-CoV-2) lineage with multiple spike mutations in South Africa. *medRxiv*, doi:10.1101/2020.12.21.20248640 (2020).

7 Yi, C. *et al.* Key residues of the receptor binding motif in the spike protein of SARS-CoV-2 that interact with ACE2 and neutralizing antibodies. *Cell Mol Immunol* 17, 621-630, doi:10.1038/s41423-020-0458-z (2020).

8 Wang, Z. *et al.* mRNA vaccine-elicited antibodies to SARS-CoV-2 and circulating variants. *bioRxiv*, doi:10.1101/2021.01.15.426911 (2021).

9 Mallapaty, S. COVID mink analysis shows mutations are not dangerous - yet. *Nature* 587, 340-341, doi:10.1038/d41586-020-03218-z (2020).

10 Baum, A. *et al.* Antibody cocktail to SARS-CoV-2 spike protein prevents rapid mutational escape seen with individual antibodies. *Science* 369, 1014-1018, doi:10.1126/science.abd0831 (2020).

11 Hodcroft, E. B. *et al.* Emergence and spread of a SARS-CoV-2 variant through Europe in the summer of 2020. *medRxiv*, doi:10.1101/2020.10.25.20219063 (2020).

12 Hou, Y. J. *et al.* SARS-CoV-2 D614G variant exhibits efficient replication ex vivo and transmission in vivo. *Science* 370, 1464-1468, doi:10.1126/science.abe8499 (2020).

13 Ku, Z. *et al.* Molecular determinants and mechanism for antibody cocktail preventing SARS-CoV-2 escape. *Nat Commun* 12, 469, doi:10.1038/s41467-020-20789-7 (2021).

14 Ledford, H. Antibody therapies could be a bridge to a coronavirus vaccine - but will the world benefit? *Nature* 584, 333-334, doi:10.1038/d41586-020-02360-y (2020).

15 Walser, M. *et al.* Highly potent anti-SARS-CoV-2 multivalent DARPin therapeutic candidates. *bioRxiv*, doi:10.1101/2020.08.25.256339 (2020).

16 Oude Munnink, B. B. *et al.* Transmission of SARS-CoV-2 on mink farms between humans and mink and back to humans. *Science* **371**, 172-177, doi:10.1126/science.abe5901 (2021).

17 Yan, R. *et al.* Structural basis for the recognition of SARS-CoV-2 by full-length human ACE2. *Science* **367**, 1444-1448, doi:10.1126/science.abb2762 (2020).

18 Callaway, E. Fast-spreading COVID variant can elude immune responses. *Nature* **589**, 500-501, doi:10.1038/d41586-021-00121-z (2021).

19 Jones, B. E. *et al.* LY-CoV555, a rapidly isolated potent neutralizing antibody, provides protection in a non-human primate model of SARS-CoV-2 infection. *bioRxiv*, doi:10.1101/2020.09.30.318972 (2020).

20 Pinto, D. *et al.* Cross-neutralization of SARS-CoV-2 by a human monoclonal SARS-CoV antibody. *Nature* **583**, 290-295, doi:10.1038/s41586-020-2349-y (2020).

21 Shi, R. *et al.* A human neutralizing antibody targets the receptor-binding site of SARS-CoV-2. *Nature* **584**, 120-124, doi:10.1038/s41586-020-2381-y (2020).

22 Starr, T. N. *et al.* Deep Mutational Scanning of SARS-CoV-2 Receptor Binding Domain Reveals Constraints on Folding and ACE2 Binding. *Cell* **182**, 1295-1310 e1220, doi:10.1016/j.cell.2020.08.012 (2020).

23 Berger Rentsch, M. & Zimmer, G. A vesicular stomatitis virus replicon-based bioassay for the rapid and sensitive determination of multi-species type I interferon. *PLoS One* **6**, e25858, doi:10.1371/journal.pone.0025858 (2011).

24 Torriani, G. *et al.* Macropinocytosis contributes to hantavirus entry into human airway epithelial cells. *Virology* **531**, 57-68, doi:10.1016/j.virol.2019.02.013 (2019).

25 Torriani, G. *et al.* Identification of Clotrimazole Derivatives as Specific Inhibitors of Arenavirus Fusion. *J Virol* **93**, doi:10.1128/JVI.01744-18 (2019).